Recognition of Molecular Planarity of Cationic Dyes by Anionic, Crystalline Bilayer Aggregates. Evidence Using Metachromatic and Solvatochromic Properties

Hiroshi Hachisako,*,[a] **Tetsuya Yamazaki,**[a] **Hirotaka Ihara,**[b] **Chuichi Hirayama**[b] **and Kimiho Yamada**[a]
[a] *Division of Applied Chemistry, Graduate School of Kumamoto Institute of Technology, Kumamoto 860, Japan*
[b] *Department of Applied Chemistry, Faculty of Engineering, Kumamoto University, Kumamoto 860, Japan*

Steric selectivity of metachromatic, cationic dyes related to molecular planarity has been investigated using a number of representative anionic bilayer aggregates described in the preceding paper. The anionic bilayer membranes specifically incorporated planar cationic dyes such as methylene blue (MB) and acridine orange (AO) as monomers in the hydrophobic region of crystalline bilayer aggregates, whereas bulky dyes such as crystal violet (CV), cyanine dye (NK-737) and rhodamine 6G (R6G) could not be incorporated and existed mostly as aggregates in the hydrophilic region. The incorporated, planar dyes underwent monomer-to-aggregate transitions during the gel-to-liquid crystalline phase transition of the bilayer host, whereas the unincorporated, bulky dyes underwent aggregate-to-monomer transitions under the same conditions. With these properties in mind, the conditions for planarity recognition of cationic dyes were investigated in relation to steric hindrance among intramolecular aromatic rings, bulkiness of substituted groups attached to the aromatic rings, and hydrophobicity. Solvatochromic dyes which ordinarily showed no aggregation were also investigated for the direct observation of the microenvironment in which the dyes exist and for the generalization of planarity recognition. It was revealed that distortion of aromatic rings caused by the steric hindrance significantly interfered with the incorporation of the dye. In a series of planar dyes with the same aromatic rings, an increase in molecular distortion by introducing bulky substituents made incorporation more difficult in spite of there being an increase in the hydrophobicity. These results indicate that complete molecular planarity, resulting from minimal distortion of aromatic rings and the absence of bulky substituents, is more important than hydrophobicity for preferential incorporation. Variations in the molecular structure of the L-glutamate amphiphiles also makes less clear the classification of dyes according to the extent of molecular packing among L-glutamate residues. An optimum molar ratio of amphiphile to dye also exists in which the selectivity between planar and hindered dyes is maximized.

Molecular recognition is one of the most fundamental and important processes in living systems. The construction and utilization of such specific and highly selective processes as artificial systems is the current target of many researchers. Synthetic bilayer membranes are some of the most attractive materials for the purpose. Dyes are convenient materials as guest molecules and microenvironmental probes owing to their useful characteristics such as aggregation, fluorescence emission, solvatochromism, thermochromism. In general, variations in the absorption spectra of dyes are not necessarily dependent only on their chemical structure. In solution, differences in absorption spectra from that of monomeric species usually depend on the nature of the solvent and the concentration. Another cause of variation in absorption spectra is electrostatic interaction with oppositely charged polyelectrolytes. This effect is termed metachromasy and, to date, a considerable number of reports have appeared.[1-25] It is generally agreed that the metachromasy is due to reversible polymerization of the dye molecules, with the polymer exhibiting an absorption spectrum different from that of the monomer.[2] It is believed that, in many cases, the aggregation of cationic dyes is restricted to dimerization,[1] although some kinds of cyanine dye form higher polymers (J-aggregates) in concentrated aqueous solution[26] and on such as silver halide.[1]

In our previous communication,[27] we reported the extraordinary monomer-to-dimer transition of MB. The detailed mechanism was determined by investigation of the variation of chemical structure of amphiphiles using MB as the guest molecule, and is described in the accompanying paper.[28] The transition was induced by the gel-to-liquid crystalline phase transition of the bilayer aggregates formed from the representative amphiphilic telomer **1** with an oligo(acrylic acid) head group and the corresponding, much simplified amphiphile **2**. These bilayer aggregates induced similar behaviour in AO[27] whose molecular structure is relatively similar to that of MB. It is especially noteworthy that the transition of MB induced by the gel-to-liquid crystalline phase transition is in the opposite direction compared with those of CV and NK-737.[27] CV and NK-737 showed ordinary aggregate-to-monomer transition in **1** systems, respectively. This means that MB and AO were selectively incorporated into anionic, crystalline bilayer aggregates of **1** and **2**, whereas CV and NK-737 could not be incorporated into the hydrophobic region but existed in hydrophilic region and aggregated as a result of electrostatic binding to carboxylates. Therefore, it is considered that the anionic, crystalline bilayer membranes formed from L-glutamate-based amphiphiles are selective not only for MB and AO but also for other cationic dyes which must have a common feature in their molecular structures. These results were an indication of molecular recognition. However, it is difficult to evaluate all the different kinds of dye systematically by using monomer-to-aggregate transition phenomena, because some of the much less planar dyes show little or no aggregation (metachromatic) properties. Therefore incorporation behaviour of such dyes into crystalline bilayers cannot be evaluated by using monomer-to-aggregate transition phenomena accompanied by gel-to-liquid crystalline phase transitions. However, if the dyes are solvatochromic, the polarity of the microenvironment can be evaluated by the change in the wavelength of the absorption maximum (λ_{max}) caused not by aggregation but by solvatochromism. Unfortunately, most of the metachromatic dyes used in this study did not show any significant solvatochromism which is generally used for probing microenvironments in which the dyes exist. Therefore, direct observations of dye incorporation and release were difficult, although the dispersion states of the dyes could be inferred by metachromatic properties alone to some extent. The other crucial problem is that various kinds of dye have different hydrophobicities which play a significant role in their hydrophobic interactions with molecular assemblies in water. In general, it is considered that the higher the hydrophobicity of the dye, the easier the dyes can be incorporated into the hydrophobic region of the molecular assemblies. Therefore, the effects of molecular structure of various dyes cannot be compared directly. To circumvent these problems, structurally related dyes, *ortho*- and *para*-type stilbazolium derivatives with different *N*-alkyl groups, namely, 4-(4-dimethylaminostyryl)-*N*-methylpyridinium iodide (St-4C$_1$), 2-(4-dimethylaminostyryl)-*N*-methylpyridinium iodide (St-2C$_1$), 2-(4-dimethylaminostyryl)-*N*-ethylpyridinium iodide (St-2C$_2$) which are not metachromatic ordinarily but which are solvatochromic were also investigated and the preliminary results have already been described.[29] The results from these metachromatic and solvatochromic properties of dyes confirmed and generalize the planarity recognition of cationic dyes by L-glutamate-based bilayer assemblies in the crystalline state. In this paper, we

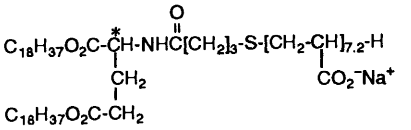

$$\underset{\underset{C_{18}H_{37}O_2C\text{-}CH_2}{|}}{C_{18}H_{37}O_2C\text{-}\overset{*}{C}H\text{-}}NH\overset{O}{\overset{\|}{C}}[CH_2]_3\text{-}S\text{-}[CH_2\text{-}\underset{CO_2^-Na^+}{CH}]_{7.2}\text{-}H$$

1

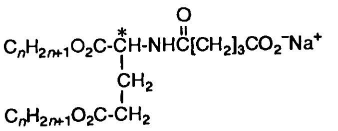

$$\underset{\underset{C_nH_{2n+1}O_2C\text{-}CH_2}{|}}{C_nH_{2n+1}O_2C\text{-}\overset{*}{C}H\text{-}}NH\overset{O}{\overset{\|}{C}}[CH_2]_3CO_2^-Na^+$$

2 $n = 18$, (L)
3 $n = 16$, (L)
4 $n = 14$, (L)
5 $n = 18$, (DL)
6 $n = 16$, (DL)
7 $n = 14$, (DL)

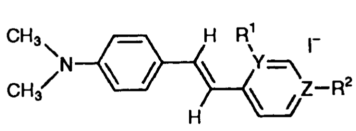

St-4C$_1$ Y = C, R^1 = H, Z = N$^+$, R^2 = CH$_3$
St-2C$_1$ Y = N$^+$, R^1 = CH$_3$, Z = C, R^2 = H
St-2C$_2$ Y = N$^+$, R^1 = C$_2$H$_5$, Z = C, R^2 = H

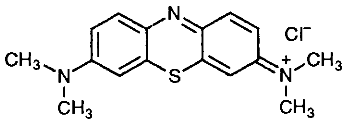

Methylene blue (MB)

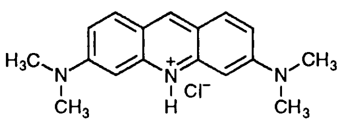

Acridine orange (AO)

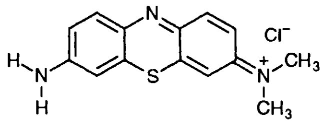

Azure A

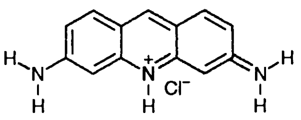

Proflavine (PF)

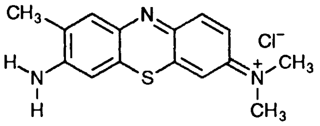

Toluidine blue O (TB)

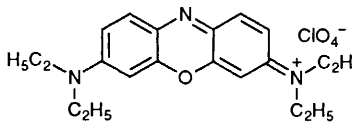

Oxazine 1 (OX)

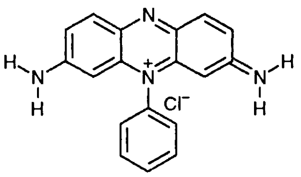

Phenosafanine (PS)

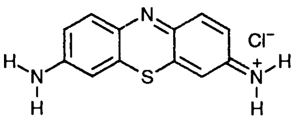

Thionine (TN)

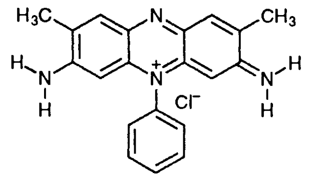

Safranine O (SO)

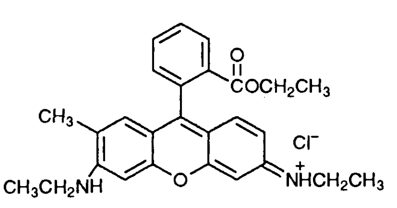

Rhodamine 6G (R6G)

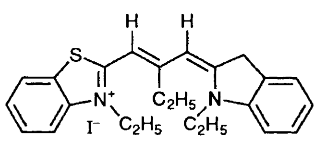

Cyanine dye (NK-737)

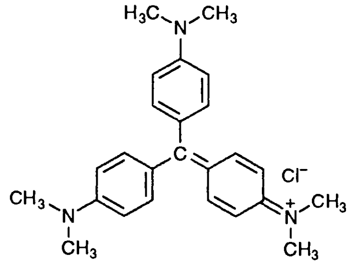

Crystal violet (CV)

describe the evidence for the planarity recognition of cationic dyes by anionic, crystalline bilayer aggregates.

Experimental

Materials.—The preparation of amphiphiles of **1** (L, $n = 18$), **2** (L, $n = 18$), **3** (L, $n = 16$), **4** (L, $n = 14$) and **5** (DL, $n = 18$) were described in the accompanying paper.[28] Amphiphiles **6** (DL, $n = 16$) and **7** (DL, $n = 14$) were newly synthesized according to the method described in the accompanying paper:[28] **6** (87%); m.p. 41–46 °C (methanol); ν_{max}(KBr)/cm^{-1} 3308, 2926, 1742, 1649, 1468 and 1205; δ(CDCl$_3$) 0.81–0.94 (t, 6 H, CH$_3$), 1.09–1.43 (m, 56 H, CH$_2$), 2.20–2.54 (m, 6 H, CH$_2$C=O), 3.92–4.30 (m, 4 H, CH$_2$OC=O). (Found: C, 71.0, H, 11.3, N, 1.95. Calc. for $C_{42}H_{79}NO_7$: C, 71.04; H, 11.21; N, 1.97%); **7** (74%); m.p. 38–45 °C (methanol) (Found: C, 69.65; H, 11.0; N, 2.18. Calc. for $C_{38}H_{71}NO_7$: C, 69.79; H, 10.94; N, 2.14%); almost the same IR and ^{1}H NMR data as for **6** were obtained. All dyes except NK-737 were purchased and used after recrystallization twice from methanol. NK-737 was donated by the Japanese Research Institute For Photosensitizing Dyes Co. Ltd. and was used without further purification. Poly(acrylic acid) (average molecular weight, 2000) was purchased from Aldrich and was used without further purification.

Lipid Membrane Preparation.—The lipids were hydrated with 30 cm^3 of deionized water at 70 °C by ultrasound (Ultrasonic generator with a 4280S type vibrator produced by Kaijyo Denki Co. Ltd.), and then the suspension was kept at 20 °C for 1 h prior to use.

Preparation of Lipid Membrane/Dye Solution.—All the solutions of the mixture of bilayer and dye were prepared by addition of a stock solution of the dye to an aqueous dispersion of the amphiphile and were sonicated. After adjusting pH to a selected value with sodium hydroxide, the solutions were used for visible absorption spectral measurements.

Assignment of Dye Species.—Assignment of monomeric and aggregated species of respective cationic dyes in the visible absorption spectra was confirmed when the following conditions were deemed to have been fulfilled. (1) When the dye solution was concentrated, the number of aggregated species increased, and conversely, dilution led to the transition from aggregates to monomers[27,30–35] (2). The number of monomeric species increased in solvents of low relative permittivity[4,35] such as alcohols. (3) The number of monomeric species increased when the aqueous dye solution was heated.[18,34,35]

For many cationic dyes in this study, it was difficult to clarify the relationships between aggregation number and their absorption maxima in the visible absorption spectra. The aggregated dye species of various cationic dyes, except MB[32,35,36] and AO[5,30] whose aggregation numbers are known or cited in the literature many times, were treated expediently as 'dimers', because the aggregation number is essentially not important at least in this study and the fact that dyes aggregate and show metachromatic behaviour by binding to carboxylates is only significant for the evaluation of incorporation and release.

Absorption Spectral Measurement.—The samples in a 1 mm quartz cell were incubated for 15 min at selected temperatures. The absorption spectra were measured with a JASCO Ubest 35 spectrophotometer.

Results and Discussion

Assignment of Dye Species in Various Media.—Assignment of the dye species in the visible absorption spectra is very important prior to investigation of the various dyes. Table 1 shows the absorption maxima (λ_{max}) of various dyes in various media. Values quoted without an asterisk denote main peaks and those with an asterisk denote shoulders or second- or higher-order peaks. To dissociate the aggregated species, methanol was used as an organic solvent of low relative permittivity.[2] In these solvents, monomeric dye species are predominant in general. To induce aggregation in cationic dyes, water, which has a much higher relative permittivity was used. By heating the aqueous solution, aggregated dye species were converted into monomers. It was also confirmed that these dyes showed no significant thermochromism in water and alcohols, if any at all. In general, absorption bands that were hypsochromically shifted compared with that of the monomeric species could be ascribed to H-aggregates with head-to-head, parallel stacking of the dye molecules.[2] In contrast, bathochromic shift could be ascribed to the J-aggregates with head-to-tail tilt stackings.[2] On the basis of these results, aggregated and monomeric dye species in various media were assigned and are denoted (D) or (M) in Table 1.

Classification of Dyes According to their Molecular Planarity.—In our previous communication,[27] we reported that MB and AO could be incorporated into the hydrophobic region of crystalline bilayer aggregates of **1**, whereas CV and NK-737 could not be incorporated and showed ordinary aggregate-to-monomer transition during the gel-to-liquid crystalline phase transition of **1**. Representative absorption spectra of **1**–AO and **1**–CV systems at 20 °C (crystalline state) and 65 °C (liquid crystalline state) are shown in Fig. 1. As shown in Fig. 1(*a*), AO cation showed a dimer band at 475 nm and a monomer band at 502 nm at 20 °C. AO exists in cationic form under these conditions (pH 9.0) because the pK_a value of the ring nitrogen in AO is approximately 10.45.[37–39] By raising the temperature, the monomeric species are converted into the dimeric species (471 nm). The existence of an isosbestic point (490 nm) indicates that the dimeric and monomeric species are in equilibrium. On the other hand, CV showed an aggregate band at 548 nm and a monomer band at 595 nm at 20 °C. By raising temperature, numbers of the aggregated species decreased and that of the monomeric species increased. However, the absorption spectra showed no isosbestic point, indicating that at least three kinds of CV species exist in the system. The absorption spectra of CV at 20 °C in Fig. 1(*b*) is similar to that of the aqueous PAA–CV system at pH 9.0, which is indicative that CV is not incorporated into the hydrophobic region of bilayer aggregates of **1** in the crystalline bilayer state. Similar phenomena were observed when NK-737 was used instead of CV. NK-737 formed J-aggregates peaks for which appeared sharply at higher wavelength (580 nm) than that of monomeric species (550 nm). In general, it is considered that J-aggregates consist of at least 3–7 dye molecules.[2,31] Therefore, it is not likely that NK-737 exists in the inner hydrophobic region of bilayer aggregates of **1**. MB and AO have planar structures, whereas CV and NK-737 experience steric hindrance between component aromatic rings. These facts suggest that the apparent selectivity shown by crystalline bilayer aggregates of **1** is derived from the molecular planarity of these cationic dyes.

Planarity Recognition Evidenced by Metachromasy: Distortion of Intramolecular Aromatic Rings.—To interpret systematically the structural features of many kinds of metachromatic, cationic dyes, the dyes were conveniently classified into three classes according to the extent of steric hindrance and bulkiness (Fig. 2). MB, Azure A, Toluidine Blue O, AO, Proflavine, Oxazine 1 and Thionine belong to class 1. Phenosafranine (PS), Safranine O (SO) and Rhodamine 6G (R6G) belong to class 2. The most distorted dyes, CV and NK-737 belong to class 3.

Table 1 Absorption maxima (λ_{max}) of various dyes in the presence of bilayer aggregates of **1** and **2** in water. [Dye] = 1.5 × 10^{-4} mol dm^{-3}, pH 9.0. An asterisk denotes higher-order peak or shoulder. Dye species: M, monomer; D, dimer; P, polymer; J, J-aggregate.

	1 ([**1**]:[Dye] = 4)					**2** ([**2**]:[Dye] = 20)					Dye alone in water				Dye alone in methanol			
	λ_{max}/nm					λ_{max}/nm					λ_{max}/nm				λ_{max}/nm			
Dye	20 °C			65 °C		20 °C			65 °C		20 °C		65 °C		20 °C		65 °C	
Methylene Blue	614 (D)	670 (M)		608 (D)	664 (M)	617 (D)	663 (M)		608 (D)	661 (M)	610 (D)	664 (M)	613 (D)	663 (M)	612* (D)	653 (M)	612* (D)	652 (M)
Acridine Orange	478* (D)	505 (M)		473 (D)	498* (M)	473* (D)	494 (M)		473* (D)	493 (M)	470 (D)	490* (M)	— —	490 (M)	— —	488 (M)	— —	488 (M)
Proflavine	443* (D)	461 (M)		443 (D)	455* (M)	449* (D)	469 (M)		442 (D)	458* (M)	434* (D)	442 (M)	434* (D)	443 (M)	— —	455 (M)	— —	453 (M)
Toluidine Blue O	556* (P)	594* (D)	637 (M)	583 (D)	631* (M)	553* (P)	593 (D)	633 (M)	585 (D)	628 (M)	589 (D)	631 (M)	600* (D)	631 (M)	585* (D)	627 (M)	584* (D)	625 (M)
Azure A	595 (D)	645 (M)		585 (D)	638* (M)	608* (D)	649 (M)		588 (D)	629 (M)	592 (D)	625* (M)	596* (D)	628 (M)	— —	626 (M)	— —	626 (M)
Oxazine 1	607 (D)	658 (M)		607* (D)	654 (M)	604 (D)	656 (M)		605 (D)	653 (M)	602 (D)	653 (M)	606* (D)	653 (M)	597* (D)	643 (M)	597* (D)	643 (M)
Thionine	565 (D)	610 (M)		558 (D)	603* (M)	478* (P)	564* (D)	604 (M)	536 (D)	600 (M)	570* (D)	597 (M)	570* (D)	597 (M)	563* (D)	600 (M)	563* (D)	598 (M)
Phenosafranine	513* (D)	536 (M)		510 (D)	526 (M)	506 (D)	528* (M)		510 (D)	525 (M)	498* (D)	518 (M)	498* (D)	518 (M)	497* (D)	527 (M)	497* (D)	525 (M)
Safranine O	505 (D)	530* (M)		503 (D)	530* (M)	502 (D)	529* (M)		512 (D)	529 (M)	505 (D)	520* (M)	502* (D)	518 (M)	500* (D)	528 (M)	500* (D)	526 (M)
Crystal Violet	547 (D)	592* (M)		560 (D)	597 (M)	563* (D)	596 (M)		563* (D)	598 (M)	550* (D)	590 (M)	550* (D)	590 (M)	556* (D)	585 (M)	556* (D)	585 (M)
Rhodamine 6G	503 (D)	535 (M)		506* (D)	534 (M)	500* (D)	530 (M)		500* (D)	527 (M)	501 (D)	526 (M)	500* (D)	526 (M)	497* (D)	527 (M)	497* (D)	527 (M)
NK-737	515* (D)	578 (J)		518* (D)	552 (M)	527* (D)	560* (M)	574 (J)	517* (D)	553 (M)	503 (D)	541 (M)	507 (D)	542 (M)	— —	545 (M)	— —	545 (M)

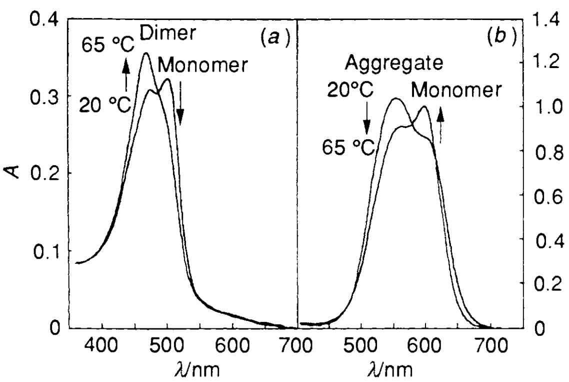

Fig. 1 Visible absorption spectra of AO (*a*) and CV (*b*) in the presence of bilayer aggregates of **1**: [**1**] = 6.0×10^{-4} mol dm^{-3}, [Dye] = 1.5×10^{-4} mol dm^{-3}, pH 9.0; Path length of quartz cell, 0.1 cm

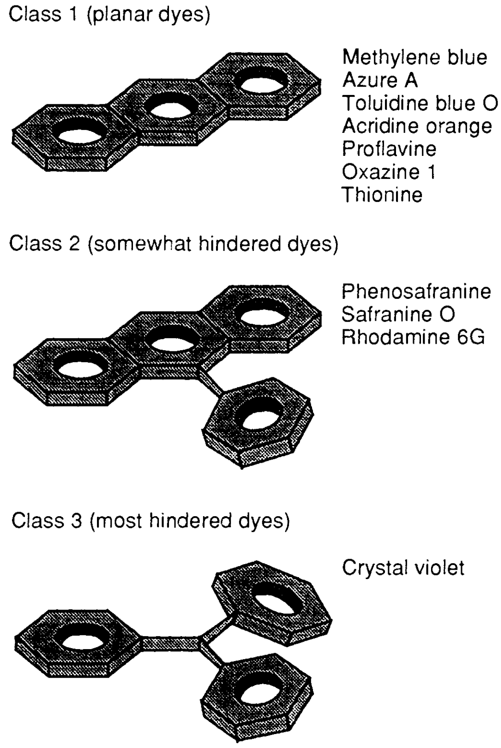

Fig. 2 Schematic representation of preliminary classification of cationic dyes according to the steric hindrance of aromatic rings

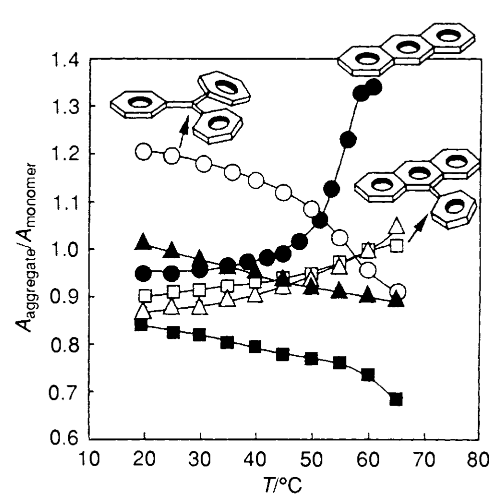

Fig. 3 Temperature dependencies of absorption ratio ($A_{dimer}/A_{monomer}$) of dyes in the presence of **1**: [**1**] = 6.0×10^{-4} mol dm^{-3}, [Dye] = 1.5×10^{-4} mol dm^{-3}, pH 9.0; ▲, poly(sodium acrylate)-CV; ■, **1**-R6G; ○, **1**-CV; △, **1**-PF; □, **1**-PS; ●, **1**-AO

However, although Malachite green (MG), which lacks only a dimethylamino group compared with CV, was originally placed in class 3, it could not be used as a substrate because it showed neither metachromatic nor solvatochromic properties.

In accordance to the classification given above, the interactions of representative dyes with anionic bilayer aggregates formed from **1** were investigated. As shown in Fig. 3, the dyes in class 1 and class 2 showed monomer-to-aggregate transition on raising the temperature, whereas CV in class 3 showed aggregate-to-monomer transition with no isosbestic point, as did the PAA–CV system, indicating that at least three dye species exist in the system. Therefore, the distinction between class 2 and class 3 was attained. However, similar distinction between class 1 and class 2 has not yet been attained.

We considered that, if bilayer aggregates with much tighter molecular packing than **1** were used instead of **1**, discrimination between class 1 and class 2 would be possible. For this purpose, the amphiphile **2** was chosen. Prior to use, it was confirmed that bilayer aggregates of **2** experienced much more difficulty in incorporating catonic dyes than those of **1** as shown in Fig. 4. In general, increasing molar ratio of amphiphile to dye promotes the transition of the dye species from aggregates to monomers by incorporating them into hydrophobic region, and the λ_{max} value reaches a constant value close to those in organic solvents.[40] Bilayer aggregates of **2** with glutarate head groups have much greater difficulty in incorporating MB than do those of telomer **1** with oligo(acrylate) head groups. Using **2**, the dyes in class 1 and class 2 were investigated at the molar ratio [**2**]/[Dye] = 15. As shown in Fig. 5(*b*), Safranine O (SO) in class 2 underwent the dimer-to-monomer transition in the presence of **2**. Conversely, the monomer-to-dimer transition was induced in the presence of **1** as shown in Fig. 5(*a*). This means that discrimination between class 1 and class 2 could be achieved in the bilayer system of **2**, therefore, the preliminary conclusion could be drawn that these bilayer aggregates have the ability to recognise planarity in cationic dyes according to the degree of distortion of the dye molecule.

Evidence for Non-incorporation of Bulky Dyes.—Next, it should be evidenced that the dyes which belong to class 3 are not easily incorporated into the hydrophobic region of anionic bilayer aggregates. As shown in Fig. 4, variation of the molar ratio of **2** to CV and R6G at fixed dye concentration did not give a critical molar ratio at which the dyes are incorporated completely. This indicates that CV and R6G cannot aggregate sufficiently and therefore, the incorporation behaviour of these dyes cannot be evaluated by use of molar ratio variations. However, R6G showed strong fluorescence at a molar ratio of 40 when the temperature was raised to bring about the liquid crystalline state of **2**. Furthermore, very weak emission was observed at 20 °C, suggesting that R6G under these conditions was not incorporated in the hydrophobic region of **2**. It was also noted that R6G continued to show weak emission when the temperature was raised to the level of the liquid crystalline state at a molar ratio of 30, at which ordinary planar dyes are incorporated almost completely, indicating that R6G is still largely unincorporated even at such a high molar ratio. As a result, bilayer membranes formed from amphiphile **2**, with its much simplified head group, cannot induce sufficient aggregation in hindered dyes such as CV and R6G. However, when telomer **1** with its oligo(acrylate) head group was used, sufficient aggregation could be induced even in both CV and R6G. Therefore, only in telomer systems such as **1** could the dispersion state of CV and R6G be evaluated by use of aggregation behaviour of these dyes in the crystalline bilayer state. In the case of NK-737, enough J-aggregates were induced

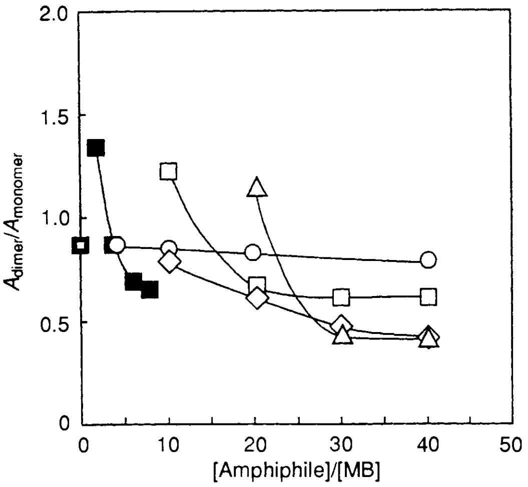

Fig. 4 Molar ratio dependencies of absorption ratio ($A_{\text{dimer}}/A_{\text{monomer}}$) of MB and bulky dyes in the presence of **1** or **2**: [Dye] = 1.5×10^{-4} mol dm^{-3} = const., pH 9.0, 20 °C; ◘, MB alone in water; ■, MB–**1**; □, MB–**2**; ○, CV–**2**; ◇, R6G–**2**; △, NK-737–**2**

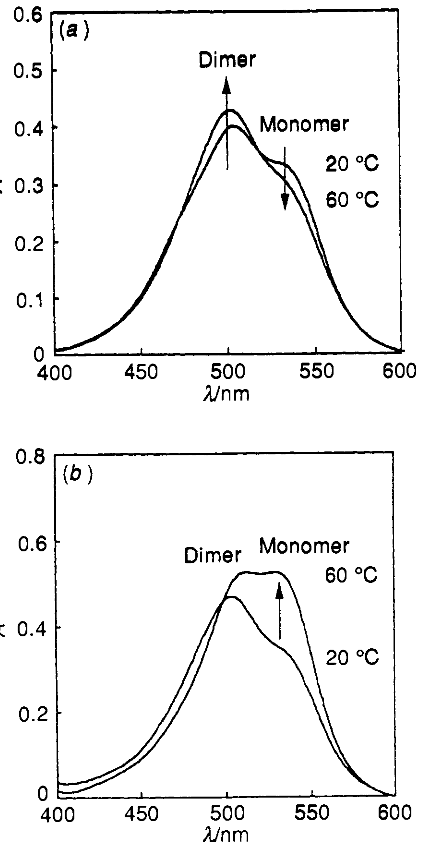

Fig. 5 Differences in the direction of transitions of dye species of SO in the presence of **1**(*a*) and **2**(*b*); [SO] = 1.5×10^{-4} mol dm^{-3}, [**1**] = 6.0×10^{-4} mol dm^{-3}, [**2**] = 2.3×10^{-3} mol dm^{-3}, pH 9.0

even in the presence of **2** in spite of the bulkiness of the dye molecule; it is known that the higher the molecular hindrance in cyanine dye molecules, the greater the tendency to form J-aggregates.[34,41] In fact, the hindered NK-737 could form J-aggregates in the presence of **2** only at temperatures below respective T_c even at the high molar ratio of 20. The J-aggregates were converted into monomeric species by the phase transition of **2**. A similar result was obtained when the molar ratio of **2** to NK-737 was increased to 30. These results clearly indicate that NK-737 is less easily incorporated into the bilayer aggregates of **2**, compared with the dyes belonging to classes 1 and 2. From the above observations that class 3 dyes do not undergo appreciable incorporation into bilayer aggregates of **1** and **2**, it is evident that molar ratio and temperature variations are not useful indicators. However, the extent of incorporation of class 3 dyes can be evaluated by fluorescence emission either spectroscopically or visually.

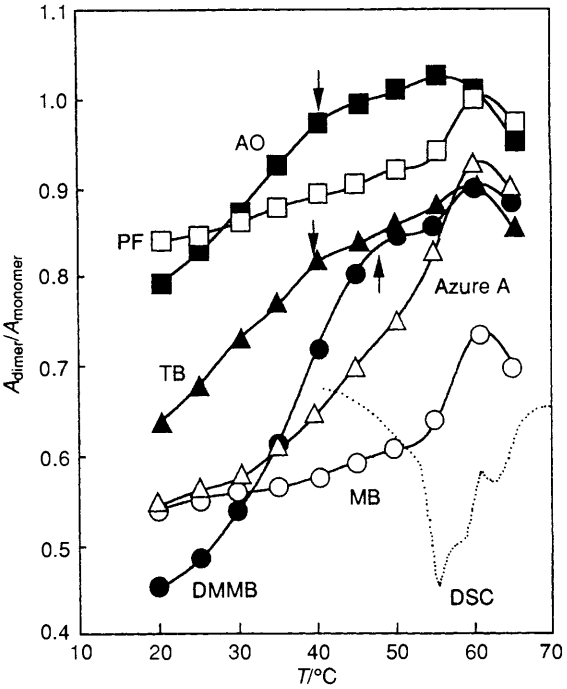

Fig. 6 Temperature dependence of absorption ratio ($A_{\text{dimer}}/A_{\text{monomer}}$) of MB, DMMB, TB, Azure A, AO and PF in the presence of **2**: [**2**] = 6.0×10^{-3} mol dm^{-3}, [Dye] = 1.5×10^{-4} mol dm^{-3}, pH 9.0. The dotted line represents the DSC thermogram of aqueous **2**.

Effect of Substituents and Hydrophobicity.—As shown in Table 2, the dyes which belong to class 2 and class 3 could be discriminated by using bilayer aggregates of **1**, as indicated by the dotted lines. However, the different behaviour shown by PS and SO still remained unclear. It was considered that the two extra methyl groups present in SO compared with PS play a crucial role in the aggregate-to-monomer transition. Therefore, the influence of bulkiness of substituents on incorporation was investigated. Three more pairs of dyes, one of which contained more substituents than the other, were chosen in addition to the pair PS–SO, namely, MB–1,9-dimethyl-Methylene Blue (DMMB), Toluidine Blue O (TB)–Azure A and AO–Proflavine (PF). According to the method given in Fig. 4, the molar ratio **2**: dye was varied. As a result, PS, MB, Azure A, and proflavine, with no methyl groups were incorporated at a lower molar ratio in spite of their somewhat lower hydrophobicity than the corresponding dyes with methyl group(s). These results clearly indicate that the presence of bulky substituted groups is an important factor that affects incorporation. It is noteworthy that DMMB and TB tend to form polymeric species. This is probably due to the difficulty in being incorporated and results in the formation of polymeric species at the surface of the crystalline bilayer membranes.

Temperature dependences were also examined, to determine whether dyes with bulky methyl group(s) are released more easily from the inner site of bilayer aggregates than those without methyl groups even at temperatures below T_c. Actually, as shown in Fig. 6, DMMB, AO and TB were easily released and aggregated at temperatures lower than the maximum temperature (T_c) of bilayer aggregation of **2**. It is noteworthy that TB showed slight polymer band[32] at a lower wavelength

Table 2 Final classification of various dyes based on the planarity recognition and the direction of transitions in the presence of bilayer aggregates of **1** and **2**, [Dye] = 1.5 × 10^{-4} mol dm^{-3}, pH 9.0

		1 ([**1**]/[Dye] = 4)		**2** ([**2**]/[Dye] = 20)	
	Dye	20 °C	65 °C	20 °C	65 °C
Class 1	Methylene Blue	Monomer ⟶ Dimer		Monomer ⟶ Dimer	
	Azure A	Monomer ⟶ Dimer		Monomer ⟶ Dimer	
	Toluidine Blue O	Monomer ⟶ Dimer (Polymer)		Monomer ⟶ Polymer ⟶ Dimer	
	Acridine Orange	Monomer ⟶ Dimer		Monomer ⟶ Dimer	
	Proflavine	Monomer ⟶ Dimer		Monomer ⟶ Dimer	
	Oxazine 1	Monomer ⟶ Dimer		Monomer ⟶ Dimer	
Class 2	Thionine	Monomer ⟶ Dimer		Monomer ⟶ Dimer	
	Phenosafranine	Monomer ⟶ Dimer		Monomer ⟶ Dimer[a]	
	Safranine O	Monomer ⟶ Dimer		Dimer ⟶ Monomer[a]	
Class 3	Crystal Violet	Dimer ⟶ Monomer		Dimer ⟶ Monomer	
	Rhodamine 6G	Dimer ⟶ Monomer		Dimer ⟶ Monomer	
	NK-737	J-aggregate ⟶ Monomer		J-aggragate ⟶ Monomer	

[a] Investigated at a molar ratio of 15 because both PS and SO showed the same behaviour (monomer ⟶ dimer ⟶ monomer transition) at a molar ratio more than 20.

than that due to dimers, when the molar ratio [**2**] : [Dye] = 20 and at a temperature lower than T_c; Azure A did not polymerize under the same conditions. The polymeric species was increased at the expense of monomeric species (monomer-to-polymer transition) at the relatively higher temperatures below T_c of **2** during the heating process. Finally, the polymeric species were converted into dimeric species at temperatures above T_c (liquid crystalline bilayer state). This result also supports the observation that the dyes with bulky substituents, in spite of having planar rings, are released at an early stage in the phase transition. On the basis of these results, it is considered reasonable that R6G which was initially classified as class 2 should actually be included in class 3 as summarized in Table 2. Therefore, it was concluded that the bilayer aggregates of **1** and **2** recognize the whole molecular planarity resulting from a combination of both lower intramolecular distortion of the aromatic rings and the low bulkiness of substituent groups.

Next, contribution of hydrophobicity to planarity recognition was considered. TB, DMMB and AO with methyl groups seem to have somewhat higher hydrophobicity than do the corresponding hydrogen-substituted dyes. In general, it is considered that the higher the hydrophobicity, the easier the dyes can be incorporated into the hydrophobic region of the bilayer aggregates. Contrary to this however, TB, DMMB and AO showed greater difficulty in being incorporated into the hydrophobic region of crystalline bilayer aggregates of **2** than did the corresponding hydrogen-substituted dyes, Azure A, MB and PF, respectively, as determined by varying the molar ratios. These contradictory results suggest therefore that specific incorporation of dyes in which the aromatic rings are the same, is influenced by the bulkiness of substituent groups. Hydrophobicity seems to exert less influence on molecular planarity, at least in these dyes, although there are some exceptions* in which hydrophobicity is still an important factor in specific incorporation. In fact, a comparison of PS and SO did not show the expected results from both molar ratio and temperature variations, probably due to their higher hydrophobicity.

Classification of cationic dyes according to the intramolecular distortion of aromatic rings and the bulkiness of substituted groups on these aromatic rings is summarized in Table 2. It is notable that the border of classification indicated by the dotted lines is also variable according to the extent of molecular packings among L-glutamate residues of the host bilayer aggregates used.

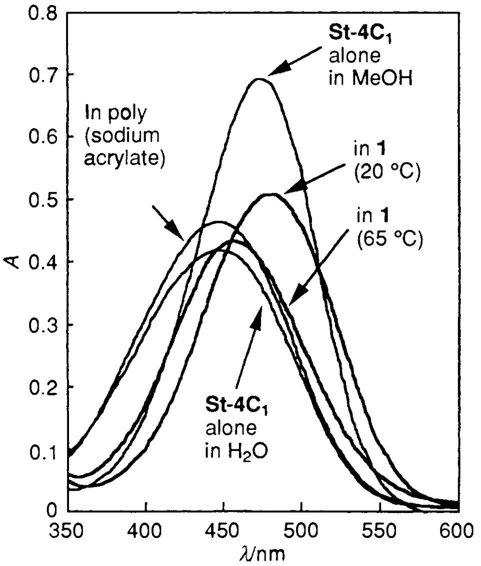

Fig. 7 Typical absorption spectra of St-4C$_1$ in various media: [St-4C$_1$] = 1.5 × 10^{-4} mol dm^{-3} = const., pH 10.0, [**1**] = 6.0 × 10^{-4} mol dm^{-3}, residue ratio of PAA to St-4C$_1$; [COO^-]/[St-4C$_1$] = 29, temperature; 20 °C and 65 °C, path length of quartz cell, 0.1 cm

Evidence by Use of Solvatochromic Dyes.—In our previous communication,[29] we described the preliminary results of planarity recognition of solvatochromic dyes St-4C$_1$, St-2C$_1$ and St-2C$_2$ by bilayer aggregates of **1**–**3**. λ_{max} of St-4C$_1$ is located at 448 nm and 477 nm in pure water and methanol respectively, regardless of temperature, as shown in Fig. 7. λ_{max} of St-2C$_1$ is located 436 nm and 462 nm in pure water and methanol, respectively, regardless of temperature. Similarly, λ_{max} of St-2C$_2$ is located 434 nm and 459 nm in pure water and methanol respectively, regardless of temperature. Therefore, the change in the site could be detected by the change in absorption maximum (λ_{max}) caused by polarity changes in the microenvironment. The solvatochromic dyes St-4C$_1$, St-2C$_1$ and St-2C$_2$

---

* In the case of PS–SO, PS was incorporated over the whole temperature range (20–65 °C) in spite of no incorporation of SO below T_c, probably due to the much higher hydrophobicity of this pair.

Table 3 Molar ratio dependences of discrimination between St-$4C_1$ and St-$2C_1$ by incorporation in the presence of bilayers **1**–**3** in the crystalline state, [Dye] = 1.5×10^{-4} mol dm^{-3} = const., pH 10.0

	Discrimination between St-$4C_1$ and St-$2C_1$			
	[amphiphile]/[dye]			
Bilayer	2	4	10	20
1	△	×	×	×
2	×	△	×	×
3	×	○	△	×

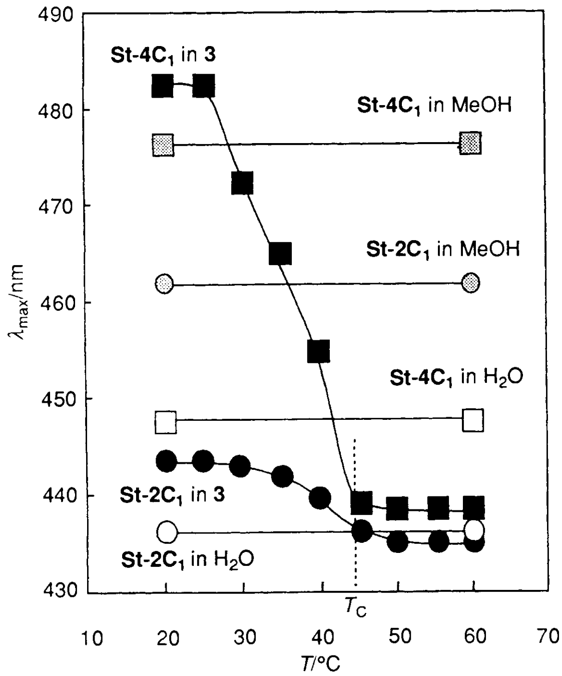

Fig. 8 Temperature dependence of λ_{max} of St-$4C_1$ and St-$2C_1$ in the presence of bilayer aggregates of **3**: [**3**] = 6.0×10^{-4} mol dm^{-3}, [St-$4C_1$] = [St-$2C_1$] = 1.5×10^{-4} mol dm^{-3}, [**3**]/[St-$4C_1$] = [**3**]/[St-$2C_1$] = 4, pH 10.0. Dotted lines indicate T_c of **3** in DSC.

have advantage of giving direct evidence of the site where the dyes are accommodated. The mechanism of selective incorporation of the planar, solvatochromic dyes could be determined clearly by this method. As shown in Figs. 7 and 8, when **3** was added to the aqueous solutions of St-$4C_1$, λ_{max} shifted to a value close to that in organic solvents such as methanol at 20 °C. Conversely λ_{max} shifted to a value close to that in water on increasing the temperature. However, St-$2C_1$, which has a ring *N*-methyl group at the 2-position and a freely rotating of pyridinium ring, is somewhat restricted owing to the steric hindrance and λ_{max} at 20 °C is very different from the value corresponding to that in methanol. This indicates that the St-$2C_1$ is harder to incorporate than is St-$4C_1$. Similar results were obtained when **2** was added to solutions of St-$4C_1$, St-$2C_1$ and St-$2C_2$ instead of **3**. However, the selectivity between St-$4C_1$ and St-$2C_1$ with regard to incorporation in crystalline bilayer hosts formed from **2** and **3** was maximized, as shown by the difference between λ_{max} of St-$4C_1$ and St-$2C_1$, at a molar ratio of approximately 4–5, as shown in Fig. 3 of ref. 29. A lower molar ratio, *e.g.*, [**3**] : [dye] = 2 led to a λ_{max} value close to that in pure water. In contrast, a much higher molar ratio led to λ_{max} values close to those in organic solvents, even though there is no λ_{max} shift from values corresponding to those in pure water in PAA–dye (St-$4C_1$, St-$2C_1$ and St-$2C_2$) systems at any residue ratio[COO^-] : [dye]. It is also notable that the selectivity tends to diminish as the molar ratio increases and reaches a value of *ca.* 10 as shown in Fig. 3 of ref. 29, and Fig. 9, indicating that both St-$4C_1$ and St-$2C_1$ were incorporated into the hydrophobic region of bilayers **2** and **3** and which showed no further selectivity. Therefore, an optimum molar ratio exists at which discrimination between planar and bulky dyes occurs. These results are summarized in Table 3. Decreasing the molar ratio amphiphile:dye to the optimum value makes the selectivity much more obvious as shown in Fig. 3 of ref. 29. However, telomer **1** did not show obvious selectivity at molar ratios of 4 and 2, the former because of complete incorporation of both St-$4C_1$ (λ_{max} = 480 nm at 20 °C) and St-$2C_1$ (λ_{max} = 468 nm at 20 °C), and, by contrast, the latter because of difficulty in incorporation of both St-$4C_1$ (λ_{max} = 466 nm at 20 °C) and St-$2C_1$ (λ_{max} = 446 nm at 20 °C). Amphiphile **2** also showed no clear selectivity even at a molar ratio of 4 because of difficulty in incorporation of both St-$4C_1$ (λ_{max} = 464 nm at 20 °C) and St-$2C_1$ (λ_{max} = 444 nm at 20 °C). Amphiphile **3** is best able to discriminate between dyes St-$4C_1$ and St-$2C_1$ as shown in Fig. 8.

The results obtained by using solvatochromic dyes support the above-described incorporation behaviour of metachromatic, planar dyes because the metachromatic dyes used in this study had limitations in that these dyes did not show enough solvatochromism to evaluate the polarity of the microenvironment and cannot evidence fully the planarity recognition by themselves. If the solvatochromic dyes St-$4C_1$, St-$2C_1$ and St-$2C_2$ showed aggregation tendencies, it would make it difficult to determine whether or not the λ_{max} change was derived only from solvatochromism. Fortunately, aggregation of St-$4C_1$, St-$2C_1$ and St-$2C_2$ was practically negligible and these dyes showed only solvatochromism. Therefore, the site where the dyes reside could be evaluated directly in various bilayer states. As a result, the hypothesis that the planar dyes such as MB and AO exist as incorporated monomers in the hydrophobic region of crystalline bilayer aggregates of **1**–**3** could be supported by using the solvatochromic, planar dye St-$4C_1$ instead of these dyes. The greater influence of molecular planarity over hydrophobicity for selective incorporation is also supported by the comparison between St-$2C_1$ (*N*-methyl type) and St-$2C_2$ (*N*-ethyl type).[29]

Dispersion States and Planarity Recognition.—In the accompanying paper[28] and previous communication,[29] it was considered that dye monomer was incorporated at a site near the glutamate residue and polar carboxylate. This consideration was supported by further investigation as shown in Fig. 10. Bilayer aggregates of **3** and **4** (L-glutamate derivatives) induced monomer-to-dimer transition in MB, whereas the corresponding DL-glutamate derivatives **6** and **7** showed quite different behaviour from those of **3** and **4**. Aggregate morphology showed no significant difference between L- and DL-derivatives.[28] A DSC thermogram showed slight differences in T_c and transition enthalpies (ΔH) between L- and DL-glutamate derivatives: **2** (L, n = 18); T_c = 55 °C, ΔH = 8.7 kcal mol^{-1}; **3** (L, n = 16); T_c = 44 °C, ΔH = 8.0 kcal mol^{-1}; **4** (L, n = 14); T_c = 28 °C, ΔH = 5.4 kcal mol^{-1}1; **5** (DL, n = 18); T_c = 60 °C, ΔH = 8.0 kcal mol^{-1}; **6** (DL, n = 16); T_c = 42 °C, ΔH = 5.9 kcal mol^{-1}; **7** (DL, n = 14); T_c = 25 °C, ΔH = 2.3 kcal mol^{-1}. It is known that the ΔH value is mainly derived from the melting of crystallized alkyl chains in the hydrophobic region. As a result, the direction of the transitions of MB in L and DL bilayer systems is quite different, indicating a difference in binding mode of MB to L- and DL-glutamate amphiphiles. It is notable that the greater the ΔH value, the more remarkable is the incorporation of MB into the crystalline bilayer state. Therefore, a correlation was observed between the ΔH value and the direction of the transition in MB species. On the basis of these results, it is strongly suggested that MB exists close to the

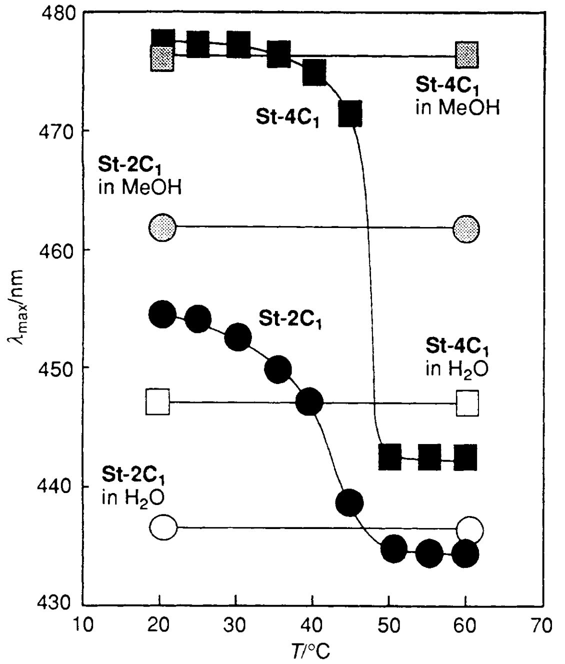

Fig. 9 Temperature dependence of λ_{max} of St-4C$_1$ and St-2C$_1$ in the presence of bilayer aggregates of 3: [3] = 1.5 × 10^{-3} mol dm^{-3}, [St-4C$_1$] = [St-2C$_1$] = 1.5 × 10^{-4} mol dm^{-3}, [3]/[St-4C$_1$] = [3]/[St-2C$_1$] = 10, pH 10.0

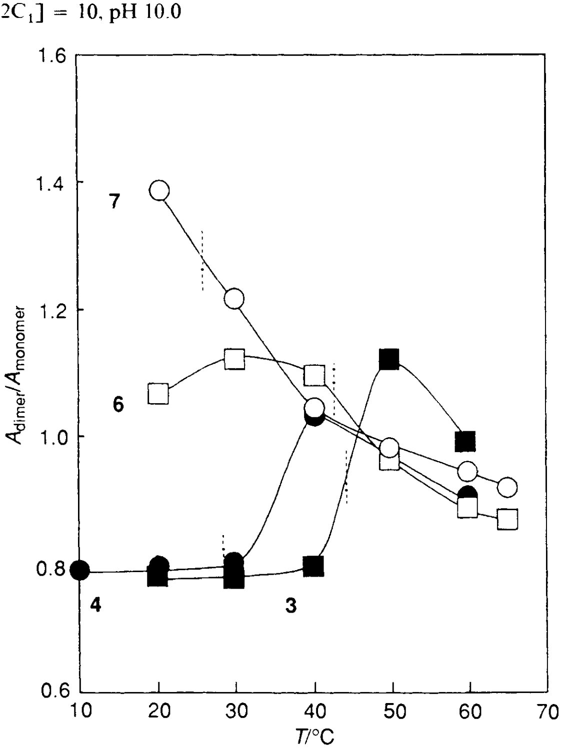

Fig. 10 Temperature dependences of absorption ratio ($A_{dimer}/A_{monomer}$) of MB in the presence of L- and DL-glutamate amphiphiles: [3] = [4] = [6] = [7] = 6.0 × 10^{-3} mol dm^{-3}, [MB] = 1.5 × 10^{-4} mol dm^{-3}, pH 10.0. Dotted lines indicate T_c in DSC.

inner site of polar surface of the bilayer aggregates. Dispersion states of planar and hindered, metachromatic dyes in bilayer **1** systems are schematically represented in Fig. 11. Planar dyes, *e.g.*, MB are incorporated into the hydrophobic region of crystalline bilayer aggregates of **1** below T_c as shown in Fig. 11(*a*). The incorporated dyes shows monomer-to-aggregate transitions on increasing temperature to T_c, and further increases in temperature above T_c lead to ordinary aggregate-to-monomer transitions of the dye species as well as the conventional dye–polyelectrolyte systems. Bulky dyes such as

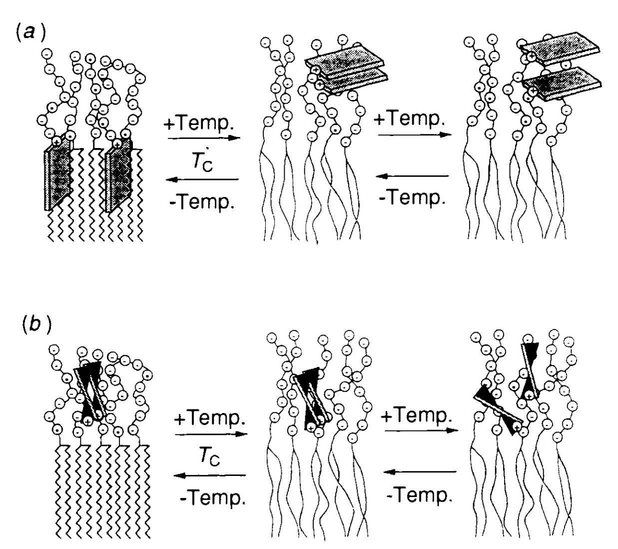

Fig. 11 Schematic representation of the dispersion states of metachromatic planar dyes such as MB (*a*) and bulky dyes such as CV (*b*) in the presence of bilayer aggregates of **1**

CV and R6G were hard to incorporate into the hydrophobic region of bilayer aggregates of **1** below its T_c as shown in Fig. 11(*b*). The H-aggregates with head-to-head stacking[2] between component dyes were gradually converted into monomeric species on raising the temperature. However, these changes are not related to the phase transition, which causes ordinary aggregate-to-monomer transitions. NK-737 formed J-aggregates with head-to-tail stacking[2] and T_c dependences in the presence of **1** and **2**. However, the interaction was essentially the same as that in Fig. 11(*b*) although NK-737 showed a T_c dependence. Similar interactions of the solvatochromic and non-metachromatic dyes St-4C$_1$ and St-2C$_1$ with bilayer aggregates of **3** are schematically respresented in Fig. 12. Similar behaviour was observed when bilayer hosts **1** and **2** were used instead of **3**.

These findings may be applicable, for example, to the separation of planar guest molecules from mixtures, and to selective chemical reactions by using planar substrates in the hydrophobic region of crystalline bilayer aggregates.

Conclusions

Anionic bilayer membranes of **1**–**3** in the crystalline state incorporate cationic dyes according to the molecular planarity regulated by the minimization of intramolecular steric hindrance between aromatic rings and of the bulkiness of substitutent groups. Molecular planarity is more important than hydrophobicity in the incorporation of the cationic dyes. Electrostatic interactions between bilayers and dyes is also one of the necessary conditions for the planarity recognition. The mode of molecular packing between neighbouring glutamate residues in bilayer aggregates is specific and influences the classification of dyes as does the molecular structure of the dyes themselves, since the interactions of the dyes with L- and DL-glutamate derivatives are quite different. The amphiphilic telomer **1** is capable of inducing sufficient aggregation in very hindered metachromatic dyes which cannot aggregate enough when bound to the bilayer **2** which has a much simplified headgroup. This leads to the obvious discrimination between non-solvatochromic, planar and hindered dyes. However, for precise discrimination of planarity such as between class 1 and class 2, telomer **1** was not suitable and amphiphile **2** was preferred. A similar conclusion was drawn when solvatochromic and non-metachromatic dyes such as St-4C$_1$ and St-2C$_1$ were used instead of the metachromatic dyes. In this case, the amphiphile **3**

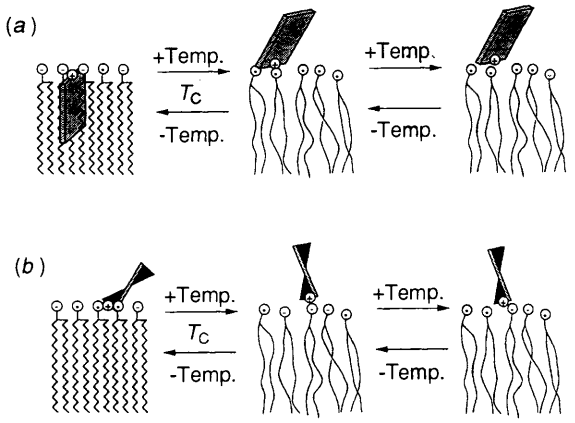

Fig. 12 Schematic representation of dispersion states of solvatochromic, non-metachromatic planar dyes St-4C_1 (*a*) and bulky dyes St-2C_1 or St-2C_2 (*b*) in the presence of bilayer aggregates of **3**

was most suitable. An optimum molar ratio of amphiphile to dye was also determined for maximum discrimination between planar and hindered dyes.

Acknowledgements

We are grateful to the Japanese Research Institute for Photosensitizing Dyes Co., Ltd. for donating the NK-737.

References

1 L. Michaelis and S. Granick, *J. Am. Chem. Soc.*, 1945, **67**, 1212.
2 A. H. Herz, *Adv. Colloid Interface Sci.*, 1977, **8**, 237.
3 G. Blauer, *J. Phys. Chem.*, 1961, **65**, 1457.
4 P. Mukerjee and A. K. Ghosh, *J. Phys. Chem.*, 1963, **67**, 193.
5 M. Hatano, M. Yoneyama and Y. Sato, *Bipolymers*, 1973, **12**, 895.
6 Y. Sato, M. Hatano and M. Yoneyama, *Bull. Chem. Soc. Jpn.*, 1973, **46**, 1980.
7 Y. Sato, M. Yoneyama and M. Hatano, *Bull. Chem. Soc. Jpn.*, 1972, **45**, 1941.
8 Y. Sato and M. Hatano, *Bull. Chem. Soc. Jpn.*, 1973, **46**, 3339.
9 G. G. Hammes and C. D. Hubbard, *J. Phys. Chem.*, 1966, **70**, 1615.
10 A. L. Stone and D. F. Bradley, *J. Am. Chem. Soc.*, 1961, **83**, 3627.
11 L. Stryer and E. R. Blout, *J. Am. Chem. Soc.*, 1961, **83**, 1411.
12 K. Bergmann and C. T. O'Konski, *J. Phys. Chem.*, 1963, **67**, 2169.
13 T. Soda and K. Yoshioka, *Nippon Kagaku Zasshi*, 1965, **86**, 1019 (*Chem. Abstr.*, **65**, 1609a).
14 T. Soda and K. Yoshioka, *Nippon Kagaku Zasshi*, 1966, **87**, 324 (*Chem. Abstr.*, **66**, 24063m).
15 A. Levine and M. Schubert, *J. Am. Chem. Soc.*, 1952, **74**, 5702, 5842.
16 M. Schubert and A. Levine, *J. Am. Chem. Soc.*, 1955, **77**, 4197.
17 M. K. Pal and M. Schubert, *J. Phys. Chem.*, 1961, **65**, 872.
18 M. K. Pal and M. Schubert, *J. Phys. Chem.*, 1963, **67**, 1821.
19 A. Levine and M. Schubert, *J. Am. Chem. Soc.*, 1952, **74**, 91.
20 N. Weissman, W. H. Carnes, P. S. Rubin and J. Fischer, *J. Am. Chem. Soc.*, 1952, **74**, 1423.
21 B. C. Myhr and J. G. Foss, *Biopolymers*, 1966, **4**, 949.
22 R. E. Ballard, A. J. McCaffery and S. F. Mason, *Biopolymers*, 1966, **4**, 97.
23 K. Yamaoka and R. A. Resnik, *J. Phys. Chem.*, 1966, **70**, 4051.
24 A. L. Stone, *Biochim. Biophys. Acta*, 1967, **148**, 193.
25 A. L. Stone and D. F. Bradley, *Biochim. Biophys. Acta*, 1967, **148**, 172.
26 G. Scheibe, *Kolloid Z.*, 1938, 82.
27 H. Hachisako, Y. Motozato, R. Murakami and K. Yamada, *Chem. Lett.*, 1992, 219.
28 Preceding paper: H. Hachisako, T. Yamazaki, H. Ihara, C. Hirayama and K. Yamada, *J. Chem. Soc., Perkin Trans. 2*, 1994, 1671.
29 H. Hachisako, T. Yamazaki, R. Murakami and K. Yamada, *Liq. Cryst.*, 1993, **15**, 723.
30 M. E. Lamm and D. M. Neville, Jr., *J. Phys. Chem.*, 1965, **69**, 3872.
31 W. West and S. Pearce, *J. Phys. Chem.*, 1965, **69**, 1894.
32 E. Braswell, *J. Phys. Chem.*, 1968, **72**, 2477.
33 S. Makio, N. Kanamaru and J. Tanaka, *Bull. Chem. Soc. Jpn.*, 1980, **53**, 3120.
34 M. Iwasaki, M. Kumagai and T. Tanaka, *Nippon Kagaku Kaishi*, 1992, 1052 (*Chem. Abstr.*, **118**, 8301z).
35 E. Rabinowitch and L. F. Epstein, *J. Am. Chem. Soc.*, 1941, **63**, 69.
36 T. Kunitake, in *Supramolecular Assemblies: New Developments in Biofunctional Chemistry*, ed. Y. Murakami, Mita Press, Tokyo, 1990, p. 17.
37 S. Massari and D. Pascolini, *Biochemistry*, 1977, **16**, 1189.
38 Y. Sato, M. Yoneyama and M. Hatano, *Bull. Chem. Soc. Jpn.*, 1972, **45**, 1941.
39 V. Zanker, *Z. Phys. Chem.*, 1952, **199**, 225.
40 N. Nakashima, H. Fukushima and T. Kunitake, *Chem. Lett.*, 1981, 1555.
41 E. S. Emerson, M. A. Conlin, A. E. Rosenoff, K. S. Norland, H. Rodriguez, D. Chin and G. R. Bird, *J. Phys. Chem.*, 1967, **71**, 2396.

Paper 3/07359I
Received 14*th December* 1993
Accepted 15*th March* 1994